European Journal of Pharmaceutics and Biopharmaceutics 142 (2019) 114–122

Contents lists available at ScienceDirect

European Journal of Pharmaceutics and Biopharmaceutics

journal homepage: www.elsevier.com/locate/ejpb

Research paper

Rational manufacturing of functionalized, long-term stable perfluorocarbon-nanoemulsions for site-specific ^{19}F magnetic resonance imaging

W. Krämer[a,*], C. Grapentin[a], P. Bouvain[b], S. Temme[b], U. Flögel[b], R. Schubert[a]

[a] Department of Pharmaceutical Technology and Biopharmacy, Albert Ludwig University of Freiburg, Freiburg, Germany
[b] Department of Molecular Cardiology, Heinrich Heine University of Düsseldorf, Düsseldorf, Germany

A B S T R A C T

Background: Perfluorocarbon (PFC)-nanoemulsions (NE) are a convenient tool for ^{19}F magnetic resonance imaging in cell and animal experiments. Typical preparation methods, like high-pressure homogenization or microfluidization, produce nanoemulsions in mL-scale. However, experiments usually require only miniscule amounts of PFC-NE, several 100 µL. For site-specific imaging tissue-specific ligands, e.g. peptides or antibodies, are covalently bound to the NE surface. This requires the use of expensive functionalized phospholipids containing reactive groups (e.g. maleimide), which often deteriorate quickly in liquid storage, rendering the manufacturing process highly cost-inefficient. A technique to manufacture storage stable NE that maintain their functionality for coupling of various ligands is desired.

Methods and results: Different PFC-NE formulations and preparation techniques were compared and the most suitable of these was tested in short-, as well as long-term stability tests. Droplet size stability was investigated by dynamic light scattering and cryogenic transmission electron microscopy over 1.5 a. Surface modifiability was assessed by a fluorescence assay. The utility of these NE was proven in an *in vitro* model.

Conclusion: The established PFC-NE platform offers a cost-efficient way to produce larger amounts of long-term storable imaging agents, which can be surface-modified on demand for application in targeted ^{19}F MRI.

1. Introduction

Surface modification of perfluorocarbon (PFC)-nanoemulsions (NE) has become a valuable tool in research involving ^{19}F magnetic resonance imaging (MRI) of cell or animal models [1,2]. While cell experiments and most animal experiments involving the use of smaller animals such as mice or rats require only miniscule amounts of PFC-NE, approximately 50 µL for cell assays and up to 200 µL for mouse experiments [3], the standard methods used to prepare PFC-NE produce several mL of PFC-NE. The main components, PFCs, are fairly expensive to manufacture and are required in substantial amounts for the preparation of PFC-NE preparation, rendering any excess product a waste of resources.

PFCs are fully fluorine substituted hydrocarbons, which can contain one or several heteroatoms. The size and structure of PFCs are varied, with both linear and cyclic PFCs available. A common feature among them is the electron dense and hardly polarizable fluorine atom shell which encloses the molecules. Furthermore C-F-bonds rank among the strongest known σ-bond in organic chemistry [4]. Those traits lead to the extreme inertness of PFCs, as well as a low intermolecular force, making them very nonpolar and often described as fluorophilic. They are also very stable towards enzymes and in biological compartments [5].

Their biological inertness paired with their high gasdissolving capacity has made them interesting substances in the search for oxygen carriers in case of severe blood loss [6]. For this purpose, PFC have to be formulated into nanoemulsions for intravenous administration. One adverse reaction which has been noted upon administration of PFC-NE are flu-like symptoms, an effect that is primarily due to the uptake of phospholipid particles by cells of the reticuloendothelial system [7]. This immune reaction has been further exploited to target circulating monocytes in the blood stream with PFC-NE. Monocytes ingest the droplets and migrate to inflammation sites, leading to a cumulation of PFC-NE in inflamed tissues [1]. ^{19}F MRI is able to delineate the raised levels of PFC and helps correlate their spatial position through the overlaying with an additional ^{1}H MR image. Possible fields of application include disease models related to inflammation processes, such as pulmonary inflammation [8], intratumoral inflammation [9], graft rejection [10] myocardial infarction [11], etc. For these applications two PFC are of special interest for research, perfluorooctylbromide (PFOB) due to its short half-life in organism of only several days, and in particular perfluoro-15-crown-5-ether (PFCE) in animal models, because of its simple ^{19}F NMR spectrum and high detectability by ^{19}F MRI [12–14].

To expand the fields of application, NE particles can be surface-modified with peptides, proteins or even small molecules to label

* Corresponding author.
E-mail address: wolfgang.kraemer@pharmazie.uni-freiburg.de (W. Krämer).

https://doi.org/10.1016/j.ejpb.2019.06.014
Received 6 March 2019; Received in revised form 29 May 2019; Accepted 13 June 2019
Available online 18 June 2019
0939-6411/

specific cells that exhibit a unique surface-target [2,15–17]. One disease model that has been shown to be accessible via surface-modified PFC-NE are venous thrombi [2]. A newer animal model entails the labeling of certain modified immune cells with PFC-NE, which have been surface-modified with GFP [16]. Surface modification is often realized by inserting already conjugated anchor molecules — mostly PEG-phospholipids or PEG-sterols — into plain PFC-NE. This process is known as the post-insertion technique (PIT) [2,18] or sterol-based post-insertion technique (SPIT) [19,20]. PIT involves the incubation of PFC-NE and anchor-ligand conjugate at 60 °C for one hour, whereas SPIT can be performed at room temperature. Therefore, PIT is a technique that is limited to ligands exhibiting sufficient stability at 60 °C. Chemical moieties used for linkage of anchor molecule to ligand include N-hydroxysuccinimide and maleimide residues. Maleimide residues offer the advantage of much greater chemical stability and therefore higher reaction specificity, limiting linking reactions primarily to thiol residues. This makes maleimide-thiol linkage a much more reliable tool for generating the desired binding of a ligand to the anchor molecule [21]. Unfortunately, even maleimide residues deteriorate after about 24 h in aqueous solution with a pH of around 7 [22]. Because of this, surface modification of PFC-NE is required just-in-time to realize sufficient labeling. However, preparation processes such as high-pressure homogenization and microfluidization, which are standard for NE manufacture, mostly involve the production of larger batch sizes of NE than needed.

A solution to this problem would be storage-stable and surface-modifiable PFC-NE, which could be prepared in advance, and then conjugated to a multitude of structures on demand. Because of the instability of maleimide residues in aqueous solutions [22], a storage method in which particle motion and therefore hydrolysis is mostly disabled must be chosen. Lyophilization is hard to accomplish for nanoemulsions due to coalescence, especially for PFC-NE since PFCs also exhibit rather high vapor pressures [5,23]. A preferable possibility would be the storage of maleimide-containing PFC-NE in a frozen state. However, the stability of such PFC-NE against freezing and thawing has not been well explored to date. To investigate the storage stability of (surface-modifiable) PFC-NE in a frozen state, the method used to determine the quality of the PFC-NE must first be clarified. Two main attributes of surface-modifiable PFC-NE may change over time: The particle size distribution may change due to coalescence or Ostwald-ripening [24,25]; and the amount of reactive maleimide residues on the particle surface may decrease due to hydrolysis [22].

As a result, the quality of surface-modifiable PFC-NE can be assessed by determining droplet size, as well as the amount of reactive maleimide residues on the NE particle surface. Particle size and morphology can be measured by dynamic light scattering (DLS) and cryogenic transmission electron microscopy (cryoTEM) [25,26], while integrity of maleimide residues on the particle surface can be measured by conjugation of those residues to a small fluorescent tag containing a reactive thiol, as in the case of 5((2-(and-3)-S-(acetylmercapto)-succinoyl)amino)-fluorescein (SAMSA-fl) [27].

A direct method for the verification of maleimide integrity on the NE surface and utility for an active targeting is the conduct of an already established thrombi model. In this cell assay utility of PFC-NE for active targeting is shown *in vitro* by ^{19}F MRI for two different peptides.

The aim of this work was therefore to develop a PFC-nanoemulsion system which is stable to freeze-thawing and which can be surface-modified on demand even after long-term storage in frozen state. In the development process we first analyzed non-pegylated and pegylated PFC-NE for their stability to freeze-thawing in two buffer systems. Secondly, we compared different methods of PFC-NE functionalization in a fluorescence assay. Finally, we assessed the short- and long-term stability of those PFC-NE, including a practical test using *in vitro* produced thrombi.

2. Materials and methods

2.1. Materials

Perfluoro-15-crown-5-ether (PFCE) (purity 99 %) and perfluorooctylbromide (PFOB) (purity 98 %) were purchased from ABCR (Karlsruhe, Germany). S75, a phospholipid blend from soy beans, and 1,2-distearoyl-*sn*-glycero-3-phosphoethanolamine-N-[methoxy(polyethylene glycol)-2000] (ammonium salt) (DSPE-mPEG(2000)) (purity 98 %) were kindly provided by Lipoid (Ludwigshafen, Germany). 1,2-Distearoyl-*sn*-glycero-3-phosphoethanolamine-N-[maleimide(polyethylene glycol)-2000] (ammonium salt) (DSPE-PEG-mal) (purity 99 %) was purchased from Avanti Polar Lipids (Alabaster, USA). 5((2-(and-3)-S-(acetylmercapto)-succinoyl)amino)-fluorescein (SAMSA-fl) was from Life Technologies (Darmstadt, Germany). Sepharose CL-4B was from GE Healthcare (Chalfont St Giles, United Kingdom).

α2-antiplasmin-derived peptide + 5(6)-carboxy-fluorescein ($\alpha2^{AP}$) and α2-antiplasmin-derived peptide with Q3 converted to A, low affinity + 5(6)-carboxyfluorescein (Q3A) were purchased from Genaxxon Bioscience (Ulm, Germany). Thrombin was obtained from Sigma Aldrich (Steinheim, Germany).

HEPES-glycerol-buffer (HGB) contained 10 mM HEPES, 280 mM glycerol; pH was adjusted to 7.0 using 2 M NaOH-solution. HEPES buffered saline (HBS) contained 10 mM HEPES, 140 mM NaCl; pH was adjusted to 7.0 using 2 M NaOH-solution

2.2. Preparation of PFC-NE

The compositions of the different PFC-NE formulations are listed in Table 1.

2.2.1. Preparation of plain PFOB-NE, PEG PFOB-NE and plain PFCE-NE

Buffer was degassed and all compounds were placed into a beaker and a crude emulsion was formed by high-shear mixing (Miccra D9 mixer with DS-8/P tool) at 21,000 rpm for 3 min. NE were further processed on a Microfluidizer M110P (Microfluidics, Westwood, USA) fitted with a F20Y 75 µm diamond interaction chamber for PFOB-NE for 9 cycles at 16,000 psi (≈1,000 bar) or on a Microfluidizer LV1 (Microfluidics, Westwood, USA) mounted with a F12Y 75 µm ceramic interaction chamber for PFCE-NE (comparison of the different functionalization methods) for 9 cycles at 24,000 psi (≈1,500 bar). During this process preparations were cooled with ice water.

2.2.2. Preparation of Mal PEG PFCE-NE and PEG PFCE-NE by direct mixing of compounds

Mal PEG PFCE-NE were prepared by previously aliquoting PEG-phospholipid components into a HPLC-vial by vacuum centrifugation of organic stock solutions, then dispersing those components with HGB by sonication for several minutes and adding the dispersion to the other components (degassed buffer) in a round-bottom centrifuge tube. NE formation was realized by high-shear mixing (Miccra D9 mixer with DS-

Table 1
Compositions of the different PFC-NE formulations used in experiments. Displayed are mass fractions in % (m/m).

formulation	PFOB	PFCE	S75	DPSE-mPEG (2000)	DSPE-PEG-mal	HGB	HBS
plain PFOB HGB	50.0	–	4.00	–	–	46.0	–
plain PFOB HBS	50.0	–	4.00	–	–	–	46.0
PEG PFOB HGB	50.0	–	3.80	0.74	–	45.5	–
PEG PFOB HBS	50.0	–	3.80	0.74	–	–	45.5
plain PFCE	–	20.0	2.66	–	–	77.3	–
Mal PEG PFCE	–	20.0	2.53	0.44	0.052	77.0	–
PEG PFCE	–	20.0	2.53	0.49	–	77.0	–

8/P tool) for 3 min at 21,000 rpm and subsequent processing on a Microfluidizer LV1 (Microfluidics, Westwood, USA) fitted with a F12Y 75 µm ceramic interaction chamber for 9 cycles at 24,000 psi for the comparison of the different functionalization methods, for 5 cycles at 16,000 psi for the short-term stability testing of Mal PEG PFCE-NE or for 7 cycles at 20,000 psi (≈1,250 bar) and a further 2 cycles at 24,000 psi for the long-term testing of Mal PEG PFCE-NE and *in vitro* thrombi targeting. While processing in LV1 the preparation was cooled with ice water.

2.2.3. Preparation of Mal PEG PFCE-NE and PEG PFCE-NE with lipid film

Mal PEG PFCE-NE were prepared by dissolving all phospholipid components (S75 + PEG-phospholipids) into chloroform and creating a homogenous lipid film through rotary evaporation. The film was dispersed with degassed HGB and added to the PFCE in a round-bottom centrifuge tube. This preparation was high-shear-mixed (Miccra D9 mixer with DS-8/P tool) for 3 min at 21,000 rpm and then processed on a Microfluidizer LV1 (Microfluidics, Westwood, USA) F12Y 75 µm ceramic interaction chamber for 9 cycles at 24,000 psi for the comparison of the different functionalization methods. While processing on the LV1 the preparation was cooled with ice water.

2.3. Freeze-thaw stability of plain PFOB-NE and PEG PFOB-NE for different buffers

To assess the resistance of PFC-NE against a cycle of freezing and thawing, four PFOB-NE were manufactured, two which contained DSPE-mPEG(2000), and two which did not; while one of each formulation contained HGB, the other HBS. All NE were aliquoted into 500 µL reaction cups at volumes of 250 µL, frozen and stored at −80 °C for 1 d in a freezer, while one sample of each was stored at 4 °C for one day as a control in a fridge. NE were thawed at 4 °C for 1 h in a fridge and particle size distributions were assessed by DLS.

2.4. Comparison of different NE functionalization methods

In order to determine the best functionalization for our PFC-NE, we compared three different methods for PEG PFC-NE: PIT, in which a plain NE is functionalized a posteriori by insertion of DSPE-PEG-mal and DSPE-mPEG(2000); the direct mixing of all compounds; and the addition of DSPE-PEG-mal and DSPE-mPEG(2000) by making of a lipid film including all lipid components.

Three 200 µL samples of plain PFCE-NE were modified by PIT and their surface modification was assessed; while the amount of reactive maleimide residues for Mal PEG PFCE-NE was assessed. Surface modification was compared by juxtaposition of f_{mal}-values, which were calculated as described for the maleimide quantification assay.

2.5. Short-term stability of frozen Mal PEG PFCE-NE

One NE (direct mixing method) was aliquoted into 500 µL reaction cups at volumes of 250 µL, and all but one sample were frozen and stored at −80 °C in a freezer. Samples were assessed with regard to particle size and content of reactive maleimide residues on the particle surface at discrete day intervals, while the first measurements were done directly post processing with freshly produced Mal PEG PFCE-NE. Thawing for subsequent days was performed by incubation at 4 °C in a fridge for 1 h.

2.6. Long-term stability of frozen Mal PEG PFCE-NE

NE (direct mixing method) were aliquoted into 500 µL reaction cups at volumes of 250 µL. One sample of each was stored at 4 °C in a fridge, whereas the others were frozen and stored at −80 °C in a freezer. Reactive maleimide residues on the NE surface were assessed for all four NE directly after preparation and for frozen samples of all four NE after 24 h and 1.5 a. Particle size was analyzed for all four NE samples stored at 4 °C after 24 h and for frozen samples of all four NE after 24 h and 1.5 a by DLS. For two of the four NE, cryoTEM analysis was used for particle size determination for storage of 24 h at 4 °C, 24 h at −80 °C, and 1.5 a at 80 °C. Reactive maleimide residues on the particle surface were compared by juxtaposing f_{mal}-values, calculated in the maleimide assay, as were particle sizes for DLS and cryoTEM analysis. Thawing was performed by incubation at 4 °C in a fridge for 1 h.

2.7. Quantification of reactive maleimide residues on NE surface

SAMSA-fl was dissolved in DMF at a concentration of 25 mg/mL. To activate the thiol an appropriate amount of SAMSA-fl solution was mixed with 100 mM NaOH at a concentration of 7 mg/mL and incubated for 15 min (pH ≈ 11). The solution was neutralized by addition of a 160 mM NaH_2PO_4 solution. 200 µL of NE were mixed with an amount of activated SAMSA solution equivalent to a 10-fold excess of SAMSA-fl to the maleimide anchor. The mixture was incubated for 2 h at 25 °C in the dark. To separate free SAMSA-fl from conjugated SAMSA-fl, size exclusion chromatography (SEC) with Sepharose CL-4B was performed. The concentration of surface-bound SAMSA-fl was measured by fluorescence spectrometry (LS55, PerkinElmer, Waltham, USA; λ_{ex} = 495 nm; λ_{em} = 512 nm; gap $width_{ex}$ = 3 nm; gap $width_{em}$ = 5 nm; T = 25 °C) with a standard addition. Phospholipid concentration was determined by Bartlett assay. The amount of reactive maleimide functionalities on NE particles was estimated by contrasting used amount-of-substance fraction of DSPE-PEG-mal to total phospholipid and measured amount-of-substance fraction of fluorescein-tagged DSPE-PEG-mal to total phospholipid after SEC. Linearity of fluorescence intensity for different fluorophore concentrations was assured by calibration curves at different PFC-NE concentrations.

To convert the concentration of reactive maleimide from the sample to the whole NE, the concentration obtained from the assay was inserted into Eq. (1):

$$f_{mal} = \frac{c_{SAMSA-fl} \cdot 100\%}{c_{PL} \cdot x_{DSPE-PEG-mal}} \cdot 100\% \quad (1)$$

$c_{SAMSA-fl}$	measured concentration of SAMSA-fl after SEC in mol/L
c_{PL}	measured phospholipid concentration after SEC in mol/L
f_{mal}	ratio of reactive maleimide residues on NE surface and used maleimide anchor in %
$x_{DSPE-PEG-mal}$	mole fraction of DSPE-PEG-mal to total phospholipid in %

2.8. Size exclusion chromatography (SEC)

Size exclusion chromatography was performed to separate surface-bound SAMSA-fl from free SAMSA-fl. Columns of 25 cm length and about 25 cm^3 volume were filled with a degassed dispersion of Sepharose CL-4B in HGB. The column was equilibrated once by application of 300 µL PEG PFCE-NE and washed with about 50 mL of HGB. For separation, 100 µL of sample were applied onto the column and eluted with HGB. The first fraction showing distinct turbidity and fluorescence was collected for further analysis of surface-bound SAMSA-fl.

2.9. Bartlett assay

Since direct PFC quantification is difficult, phospholipid concentration was used as a marker for dilution of NE. To assess the phospholipid concentration after SEC, a Bartlett assay was performed. The assay is based on a complexation of molybdenum and phosphate stemming from incinerated phospholipids of the sample [28].

NE samples equivalent to about 100–200 nmol total lipid were pipetted into phosphate-free round-bottom centrifuge tubes. Samples were incinerated after addition of 500 µL of 10 N sulfuric acid at 160 °C for 3 h. Next, 1 mL of 30 % (V/V) H_2O_2 solution was added and incubated for an additional 4 h at 160 °C. After addition of 0.2 mL of an aqueous solution of Fiske-Subbarow reducer (14.6% m/V) and 4.5 mL of an aqueous ammonium molybdate solution (0.22 % m/V), samples were incubated for a further 10 min at 95 °C in glass tubes. Absorption of the resulting complex was measured at 830 nm wavelength and evaluated by a calibration curve of K_2HPO_4.

2.10. Post-insertion technique (PIT)

A solution of DSPE-PEG-mal and DSPE-mPEG(2000) (molar ratio 5:95) in HEPES-glycerol-buffer was conjugated with a 10-fold amount of activated SAMSA-fl for later quantification. 200 µL of plain PFCE-NE were incubated with an amount of this solution approximately equivalent to an amount of PEG-phospholipid present in Mal PEG PFCE-NE for 1 h at 60 °C. NE particle separation from free SAMSA-fl and non-embedded PEG-phospholipids, as well as quantification of surface-bound SAMSA-fl, was performed as previously mentioned.

2.11. Dynamic light scattering (DLS)

For assessment of NE particle size distribution, DLS was used. NE samples were diluted (1:200 V/V) and measured on a Zetasizer Nano ZS (Malvern Instruments, Malvern, UK). Measurements were performed at 25 °C, after 3 min of equilibration at a scattering angle of 173 ° and wavelength of 633 nm. The autocorrelation signal was evaluated by cumulant analysis and z-average (intensity-weighted hydrodynamic particle size) as well as polydispersity index (pdi; representing size distribution width) were calculated. All measurements were performed in triplicate and averaged for a single value.

2.12. Cryogenic transmission electron microscopy (cryoTEM) analysis

NE were diluted 1:5 or 1:10 with HGB. Five µL of diluted NE were applied onto a 400 mesh Quantifoil® S7/2 perforated carbon film on copper grids (Quantifoil Micro Tools GmbH, Jena, Germany). Excess liquid on the grid was removed with filter paper and the sample immediately shock-frozen by injection into liquid ethane. Sample preparation was performed using a CryoBox 340719 (Carl Zeiss, Oberkochen, Germany) in a climate-controlled room. Successive grid fixation on the sample rod (626-DH, Gatan, Warrendale, USA) and rod transfer into the transmission electron microscope (TEM; Leo 912 Omega, Carl Zeiss, Oberkochen, Germany) were conducted in a N_2 atmosphere at a temperature of 90 K [29]. TEM was operated at 120 kV for the acquisition of images (Camera: Proscan HSC 2, Oxford Instruments, Abingdon, USA) with a 6,300- to 12,500-fold magnification.

For particle size assessment an overview image of one grid hole was divided into several detailed images, including a significant amount of NE particles for analysis [30]. NE droplets can be distinguished as dark circles, while liposomes appear as light rings. [25,31]. NE droplet diameter was determined using iTEM 5.0 (Build 1054) software (soft imaging System GmbH, Münster, Germany). Diameters of all NE particles on one grid hole were measured and results compiled in the form of box plots presenting median-, d_{p25}-, d_{p75}-, d_{p05}-, d_{p95}-, d_{p01}-, and d_{p99}-values [25].

2.13. In vitro targeting of thrombi

Mal PEG PFCE-NE and PEG PFCE-NE were aliquoted into 500 µL reaction cups at volumes of 250 µL, stored at −80 °C in a freezer for 30 days and then thawed by incubation for 1 h at 4 °C in a fridge. Next, samples of both preparations were each conjugated once to either Q3A or $\alpha2^{AP}$ by incubation at 25 °C for 120 min. $\alpha2^{AP}$ is stably incorporated into thrombi during their formation by cross-linkage at its Q3 glutamine. Particles displaying this peptide should therefore be incorporated into acute thrombi. Q3A lacks the Q3 glutamine and exhibits an alanine in its place, therefore there should be no incorporation in acute thrombi. Surface modification with peptides is displayed by affinity to acute thrombi. Human blood was obtained from two healthy volunteers by venipuncture with a 21 gauge needle and anticoagulated with 10 % (m/m) citric acid. Samples were mixed before further treatment. Next, blood was centrifuged at 150 g for 10 min to generate platelet rich plasma. One mL of platelet rich plasma was incubated with 100 µL of a solution of thrombin (5 $U * mL^{-1}$), 5 µL of a solution of ADP (1 mM) and 100 µL of a solution of $CaCl_2$ (0.4 M) in PBS. Volumes of 130 µL of this mixture were promptly transferred into a 96-well plate, 10 µL of conjugated NE preparation was then added to each well and incubated for 15 min at 37 °C on a shaker. The resulting thrombi were extracted and washed eight times with PBS containing Ca/Mg.

$\alpha2^{AP}$ affinity to thrombi was verified by fluorescence measurement employing an IVIS Lumina II imaging system (PerkinElmer, Waltham, USA) after placement of washed thrombi on a glass plate with some buffer (excitation time: 0.5 s, λ_{ex} = 488 nm, emission-filter: Cy5.5, binning: medium, F-stop = 8, FOV = A). NE particle incorporation into thrombi was assessed by ^{19}F MRI using a 9.4 T Bruker AVANCE^{III} Wide Bore nuclear magnetic resonance spectrometer (Bruker, Rheinstetten, Germany). In addition to ^{19}F signals, ^{1}H signals were measured separately and overlaid with ^{19}F signals for visualization. ^{1}H signals were measured at 400.21 MHz (TR = 3500 ms, RARE factor: 16, FOV = 2.00 × 2.00 cm^2, matrix: 128 × 128, slice thickness: 1 mm, scan-time: 1 min). ^{19}F signals were determined at 376.54 MHz (TR = 2500 ms, RARE factor: 32, FOV = 2.00 × 2.00 cm^2, matrix: 32 × 32, slice thickness: 1 mm, acquisition time: 5 min) [3].

3. Results and discussion

3.1. Freeze-thaw stability of plain PFOB-NE and PEG PFOB-NE for different buffers

To evaluate the impact of two different buffers and pegylation on the freeze–thaw stability of PFC-NE an initial study of different PFOB-NE formulations was performed. PFOB was chosen as model PFC, since it exhibits higher vapor pressures than for example the experimentally important PFCE. The higher Ostwald-ripening tendency of the PFOB droplets attributable to this higher vapor pressure makes PFOB a more challenging compound for NE formulation. One batch of each formulation were prepared and four samples of each batch were frozen at −80 °C in the freezer separately to gain insight into the effect on particle size distribution and reproducibility thereof.

Formulations showed initial particle sizes (z-average) and pdi values of 151 nm/0.09 (plain PFOB HGB-NE), 145 nm/0.11 (PEG PFOB HGB-NE), 170 nm/0.20 (plain PFOB HBS-NE) and 133 nm/0.14 (PEG PFOB HBS-NE) after processing. Particle sizes (z-average) after storage for 1 d at 4 °C ranged from 172 nm to 180 nm with polydispersity indices from 0.10 to 0.20 for all formulations (Fig. 1). The plain PFOB HBS-NE showed a higher polydispersity index (pdi) than the other NE. After storage at −80 °C for 1 d, particle size (z-average) rose noticeably for plain PFOB HGB- and even more for plain PFOB HBS-NE. Pdi increased for both formulations to approximately the same mean value with greater variance for the plain PFOB HBS-NE formulation. PEG PFOB HGB-NE and PEG PFOB HBS-NE showed only slight changes in z-average and polydispersity. Both pegylated formulations showed smaller variance of particle sizes as well as polydispersity indices than the respective non-pegylated formulations.

Based on these measurements addition of DSPE-mPEG(2000) seemed to stabilize NE particles and lead to higher resilience of particles against the stress of the freezing and thawing process. Plain PFOB-NE without addition of DSPE-mPEG(2000) showed instability regarding particle size upon freezing and thawing. This instability effect was even

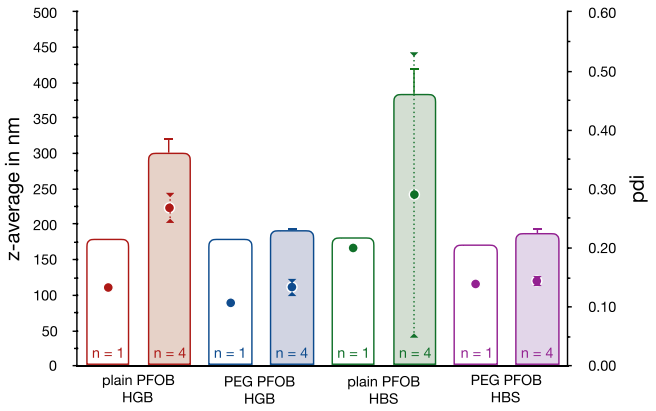

Fig. 1. Droplet size of PFOB-NE before and after freezing/thawing at −80 °C/4 °C measured by DLS. Bars represent z-average values on the left y-axis in nm, while dots indicate polydispersity indices on the right y-axis. Different formulations are indicated by differing colors, with hollow bars depicting values of NE stored at 4 °C for 1 d and filled bars depicting values of NE samples stored at −80 °C for 1 d. Error bars represent calculated standard deviations Each formulation was prepared once and four samples of each were subjected to the storage process at −80 °C with consecutive thawing at 4 °C to compare solely the effect of the freeze-thawing and exclude the influence of batch differences.

greater for the higher ionic strength HBS than for the HGB, which might be attributable to a change in ζ-potential of NE particles. The greater particle size for plain PFOB HBS-NE particles which were not freeze-thawed could be attributed to a leveled ζ-potential as well. The stabilizing effect of DSPE-mPEG(2000) was likely a steric effect [32,33]. For coalescence of NE particles, a compact film must first be formed, which requires droplets to get in close contact with each other. The PEG chains enveloping the PEG PFOB-NE particles keep them in check, inhibiting coalescence. The small sample variance of the freeze-thawed samples indicated a well reproducible freezing and thawing process for PEG PFC-NE, which was realized by simple incubation at −80 °C and 4 °C. For these reasons, PEG-coated PFC-NE with HGB as a buffer system were selected as the platform to use for further development. Since PFCE is the most commonly used PFC in cell and animal experiments, it was used for all subsequent investigations.

3.2. Comparison of different NE functionalization methods

Different functionalization methods were compared using a fluorescence assay involving SEC and phospholipid quantification (Fig. 2A). Measurements of two calibration curves of SAMSA-fl in two diluted NE both showed proportionality between fluorescence intensity and concentration of SAMSA-fl (Fig. 2B). However, the higher NE concentration led to decreased sensitivity of the measurement, as indicated by the

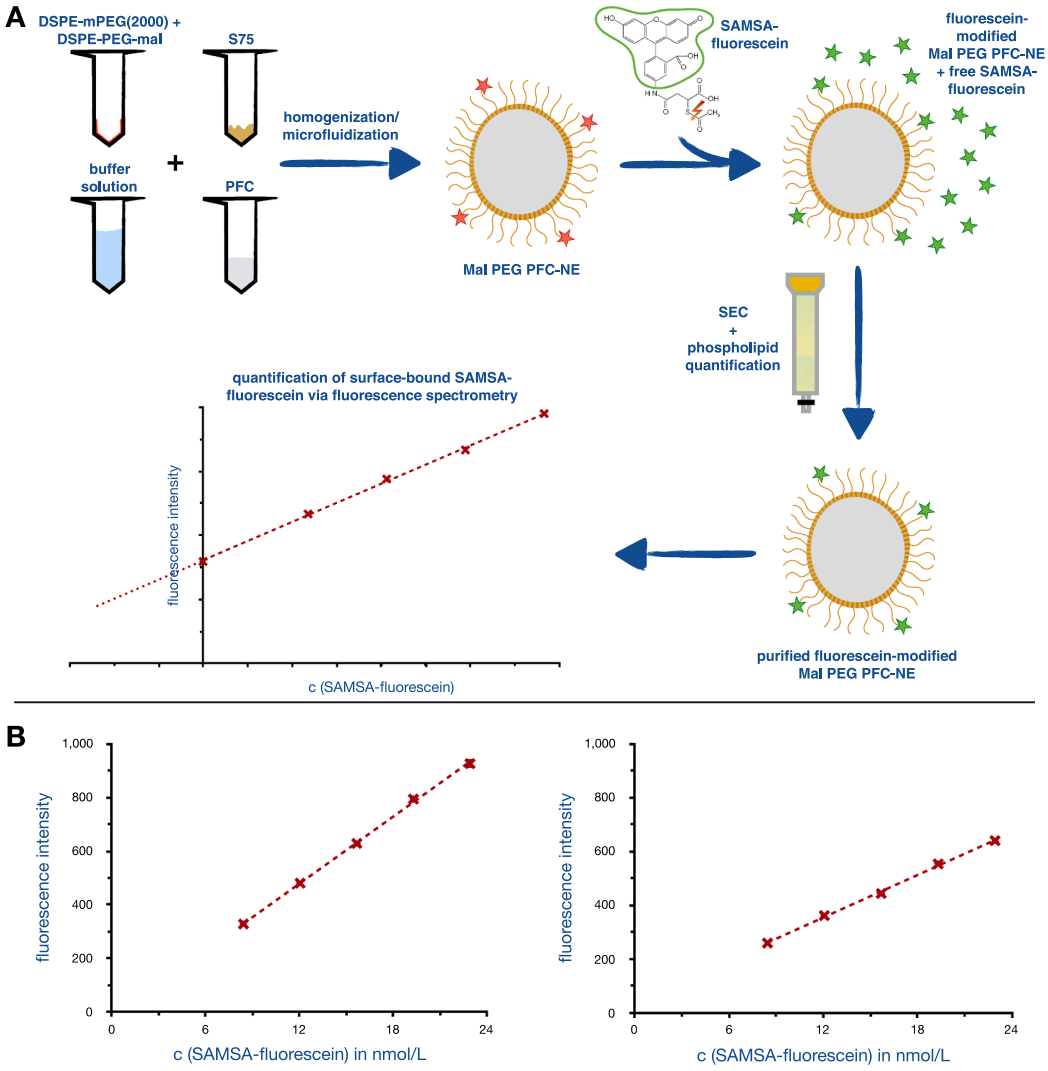

Fig. 2. A. Sketch of the DSPE-PEG-mal quantification assay. B. Concentration curves of SAMSA-fluorescein in PFOB-NE diluted with buffer 1:20 (left plot) and 1:5 (right plot).

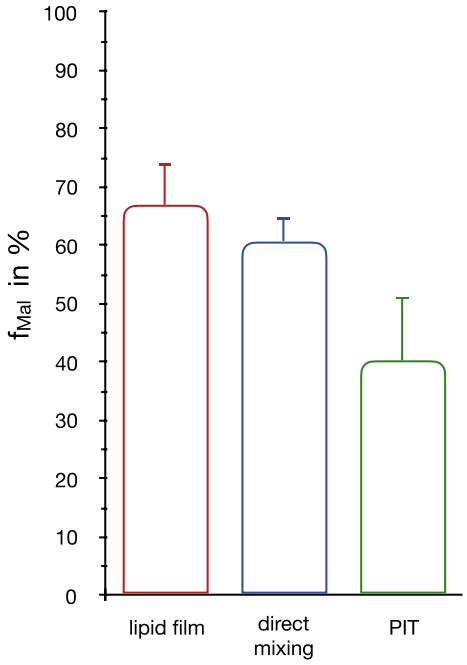

Fig. 3. Surface modifiability of the different preparation methods for PFC-NE juxtaposed as f_{Mal}-values in %. Higher values indicate higher surface modifiability of NE-particles with 100 % indicating a surface modification corresponding to 100 % used maleimide-phospholipid. Error bars represent calculated standard deviations (n = 3).

flatter slope of the curve. For the subsequent f_{mal}-measurements, PFC-NE were diluted about 1:100, minimizing this effect.

The amounts of reactive maleimide residues on the NE surface ranged from about 40 to 67 % of used DSPE-PEG-mal (Fig. 3). The preparation method involving the incorporation of the DSPE-PEG-mal and DSPE-mPEG(2000) into a homogenous lipid film containing all phospholipid components showed the highest f_{mal} with about 67 %; while the preparation method, in which a dispersion of DSPE-PEG-mal and DSPE-mPEG(2000) were only added to the weighed in PFCE and S75, showed an f_{mal} of about 61 %. The lowest f_{mal}-value of 40 % was exhibited by the PIT preparation, in which already conjugated DSPE-PEG-mal and DSPE-mPEG(2000) were inserted into plain PFCE-NE by incubation at 60 °C. Sample variance was highest for PIT and lowest for direct addition without homogenous lipid film.

These findings suggested that DSPE-PEG-mal could be incorporated into NE without a homogenous lipid film before NE processing, while maintaining reactivity of maleimide residues. The lipid film and direct mixing methods even seemed superior to the PIT method, not only in the amount of surface modification per DSPE-PEG-mal used, but also in the reproducibility of the results. The difference of about 6 % between the film method and the direct mixing method was relatively small, whereas there was a great difference in preparation effort between the two methods, with the direct mixing method easier to carry out. A possible explanation for this could be the short sonication step, which was performed in the direct mixing method. This sonication could have enhanced the hydrolysis of maleimide residues slightly. If the making of a homogenous lipid film facilitated incorporation of DSPE-PEG-mal into PFC NE particles, the effect would very likely have been small, while the solvent usage requirement and effort were clearly higher. For economic and safety reasons, the direct mixing method seemed the most promising and was therefore used for further investigations.

3.3. Short-term stability of frozen Mal PEG PFCE-NE

The short-term stability of Mal PEG PFCE-NE was investigated for a single NE batch over the course of 27 d by DLS and SAMSA-fl assay. NE droplet size quickly rose from a post processing size of approximately 130 nm to about 150 nm, but over the course of 27 d the frozen NE showed stable droplet size and low polydispersity index of around 0.1 (Fig. 4A). No prominent NE droplet deterioration could be observed. The droplet size change after two days was very likely due to establishment of system equilibrium after NE preparation, likely caused by Ostwald-ripening.

Reactive maleimide residues on the NE surface showed only minute fluctuations (Fig. 4B). These fluctuations could have been attributed to small differences between the different aliquots of the NE batch as well as random deviations due to the assay. Maleimide residues appeared stable over time for the frozen NE, owing to a reduction of diffusion and therefore hydrolysis of maleimide, which is based on particle collision [22].

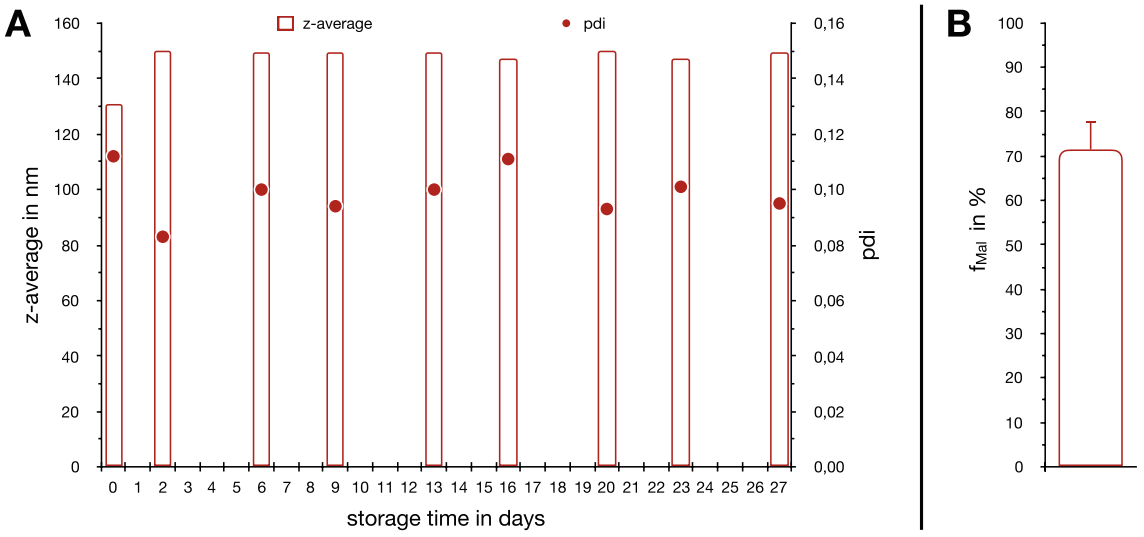

Fig. 4. A. Droplet size of a single Mal PEG PFCE-NE batch over the course of a 27 d storage period as measured by DLS. Bars represent z-average values on the left y-axis in nm, while dots depict polydispersity indices on the right y-axis. B. Surface modifiability of a single Mal PEG PFCE-NE batch over a 27 d storage period at −80 °C as f_{Mal}-value in %. Because the surface modifiability remained stable and showed no trending, it is shown as a single bar. Higher values indicate higher surface modifiability of NE particles with 100 % indicating a surface modification corresponding to 100 % of the maleimide-phospholipid used. Error bar indicates calculated standard deviation (n = 9).

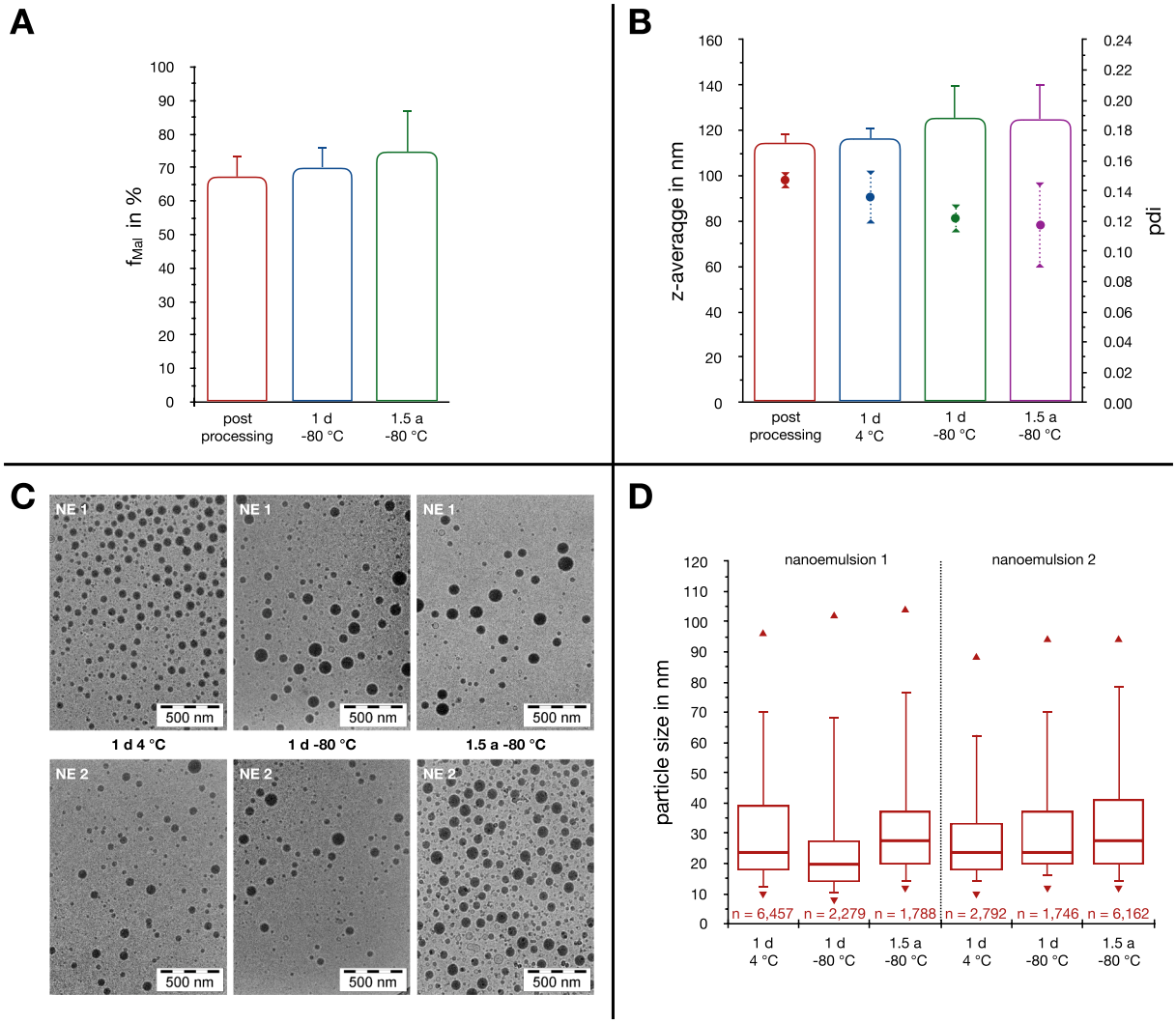

Fig. 5. A. Surface modifiability of four Mal PEG PFCE-NE batches post processing, after storage for 1 d and 1.5 a at −80 °C juxtaposed as f_{Mal}-values in %. Higher values indicate higher surface modifiability of NE particles, with 100 % indicating a surface modification corresponding to 100 % of the maleimide-phospholipid being used. Error bars represent calculated standard deviations (n = 4). B. Particle size distribution of four Mal PEG PFCE-NE batches post processing, after storage for 1 d at 4 °C, and for either 1 d or 1.5 a of storage at −80 °C as measured by DLS. Bars represent z-average values on the left y-axis in nm, while dots indicate polydispersity indices on the right y-axis. Error bars represent calculated standard deviations (n = 4). C. Images of the two Mal PEG PFCE-NE batches examined with cryoTEM for 1 d of storage at 4 °C, 1 d of storage at −80 °C and 1.5 a of storage at −80 °C. D. Particle size distributions of two Mal PEG PFCE-NE batches post processing, after 1 d of storage at 4 °C and for either 1 d or 1.5 a of storage at −80 °C according to cryoTEM. Top and bottom box caps represent d_{P75}- respectively d_{P25}-values, bar dividing line represents median-values, whiskers represent d_{P95}- respectively d_{P05}-values; d_{P99}- and d_{P01}-values are represented by top and bottom triangles.

3.4. Long-term stability of frozen Mal PEG PFCE-NE

For the long-term stability investigation of Mal PEG PFCE-NE the particle size and surface modifiability of four different batches of the same formulation were assessed for a total time span of 1.5 a. DLS data showed that z-average values of NE were around 110 nm with a polydispersity index of approximately 0.15 post processing (Fig. 5B). After storage for 1 d at 4 °C the NE droplet size remained stable, whereas the variation in polydispersity index between samples increased. NE droplet size after storage for one day at −80 °C was elevated slightly, with an increase in sample variance (n = 4). The mean polydispersity index decreased slightly to approximately 0.12, while sample variance diminished. After 1.5 a of storage NE droplet size and average polydispersity remained stable, while the sample variance of polydispersity increased.

Qualitative observation of cryoTEM images of both NE showed no major change in particle morphology from one day of storage at 4 °C to storage at −80 °C for 1 d or 1.5 a (Fig. 5C). Quantitative analysis of NE particle size revealed average median particle sizes of around 25 nm which remained constant over the course of 1.5 a. Particle size distribution did not increase considerably with d_{p99}-values of about 105 nm (NE1) and 95 nm (NE2), respectively (Fig. 5D). DLS and cryoTEM data suggested that NE remained stable over the course of 1.5 a upon storage at −80 °C and subsequent thawing with no major change in particle morphology or size distribution. The difference between particle size measurements between DLS and cryoTEM lies in the nature of these methods, with DLS overrepresenting large particles according to their scattering intensity, which is proportional to the sixth power of particle size, and measures hydrodynamic particle sizes, while cryoTEM gives an overview of actual particle shape.

Amount of reactive maleimide residues on the NE surface did show average f_{mal} of 67 % for post processing, 70 % after storage for one day at −80 °C and 75 % after storage for 1.5 a at −80 °C with a slight change in sample variance for NE after 1.5 a of storage (Fig. 5A). The differences may have been caused by differences between the NE sample aliquots and random deviations in the assay. The maleimide

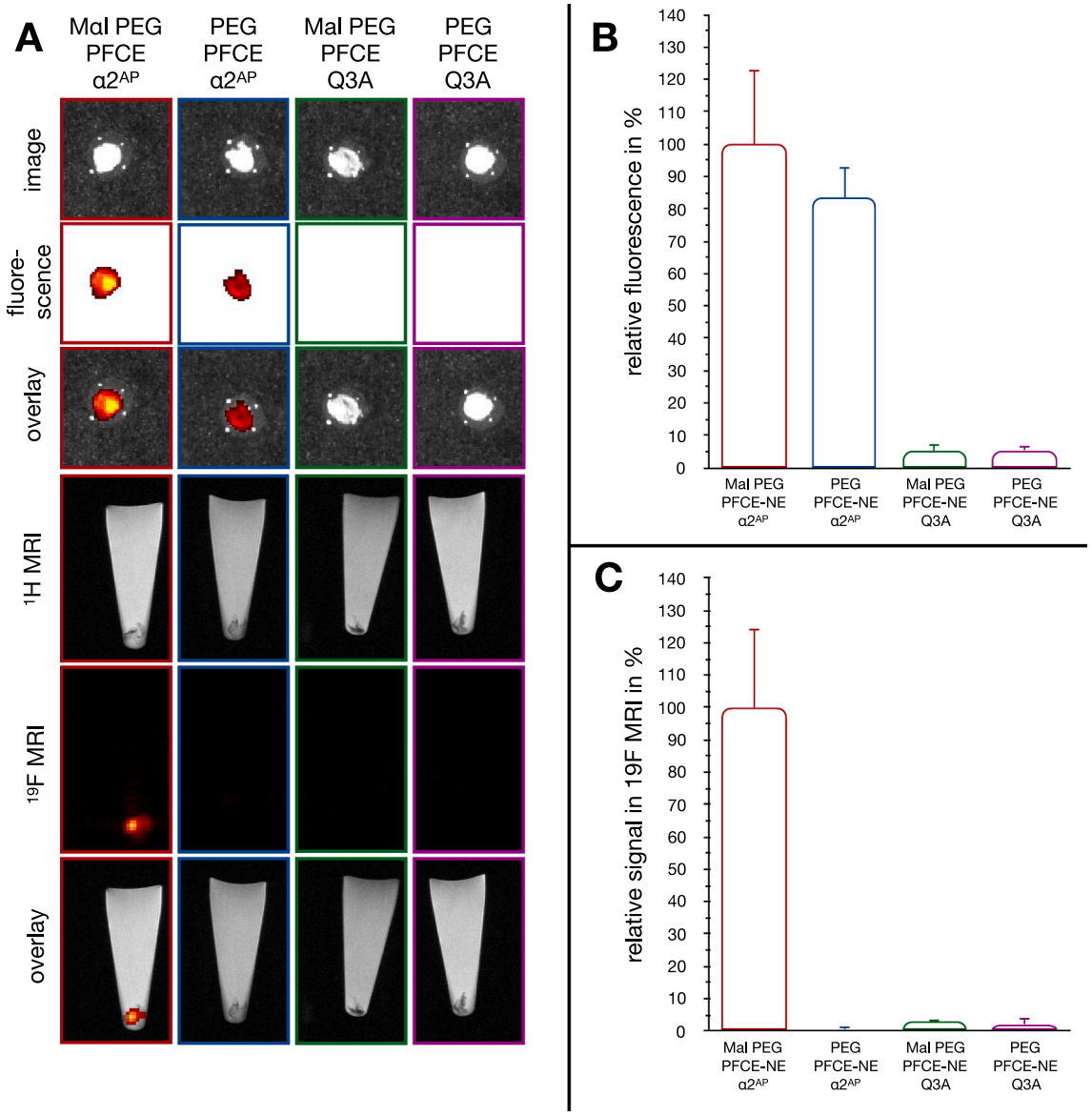

Fig. 6. A. Images, fluorescence images, fluorescence image overlays as well as ^{1}H MR, ^{19}F MR images and ^{1}H/^{19}F MRI overlays of thrombi that were treated with two different PFC-NE formulations and incubated with either α2^{AP} or Q3A. Signals in the fluorescence images indicate attachment of fluorescence-labeled α2^{AP} or Q3A, while signals in the ^{19}F MR images register presence of PFCE-NE particles in thrombi. Fluorescence images were acquired by IVIS measurements. B. Relative fluorescence values of thrombi that were treated with two different PFC-NE formulations incubated with either α2^{AP} or Q3A. Error bars indicate calculated standard deviations (n = 3). Data were acquired by IVIS measurements. C. ^{19}F MRI signals of thrombi that were treated with two different PFC-NE formulations incubated with either α2^{AP} or Q3A. Error bars represent calculated standard deviations (n = 3).

residues on the NE surface seemed to remain stable over the course of 1.5 a and could be conjugated as well as post processing.

3.5. *In vitro targeting of thrombi*

Thrombi showed strong peptide fluorescence signal for treatment with both Mal PEG PFCE-NE and PEG PFCE-NE incubated with α2^{AP} (Fig. 6A, B). Thrombi treated with Mal PEG PFCE- and PEG PFCE-NE which were incubated with Q3A showed nearly no peptide fluorescence. Because α2^{AP} and Q3A were not separated from NE, the presence of a fluorescence signal showed in any case an incorporation of at least the respective peptide into thrombi, without evidence of PFC-droplet incorporation. In conclusion, Q3A exhibited no incorporation into thrombi, while α2^{AP} did. ^{19}F MRI showed strong signals for thrombi treated with Mal PEG PFCE-NE and incubated with α2^{AP}, whereas all thrombi treated with other formulations yielded nearly no signal whatsoever. This provided evidence that only Mal PEG PFCE-NE droplets incubated with α2^{AP} bound in major fashion to the thrombi. PFC-NE lacking the maleimide residues showed almost no signal, even though they were incubated with α2^{AP} — thereby demonstrating the integrity of maleimide residues of Mal PEG PFCE-NE over a storage period of one month (Fig. 6A, C).

In summary, thrombi data suggested that Mal PEG PFCE-NE droplets maintain their conjugable attributes for an active targeting over the course of one month and provided strong signals in an established test model [2], while particles lacking any maleimide residues showed none of these traits.

4. Conclusion

Our PFC-NE containing PEG-phospholipids showed droplet size stability while frozen over a long period of time. Plain PFC-NE lacking

any PEG-phospholipid content showed changes in droplet size during the freezing/thawing process, which was proven within the scope of a small study of different PFOB-NE formulations. The direct incorporation of maleimide-containing PEG-phospholipids seems to be a reliable method for preparation of surface-modifiable PFC-NE. Only slight differences between the film method and the direct mixing method could be observed. The often-used PIT showed inferior reliability in comparison to the direct incorporation of DSPE-PEG-mal when using the same amount of DSPE-PEG-mal. Particle size distribution, as well as integrity of maleimide residues, remained stable for storage at −80 °C for PEG-phospholipid containing PFCE-NE. This stability was shown for a long time span of 1.5 a and may remain constant over an even longer period of time. In addition to the results of the SAMSA-fl assay, integrity of maleimide over a time span of one month as well as utility in a physiological active targeting assay to visualize acute human thrombi by $^{1}H/^{19}F$ MRI were demonstrated.

These findings render this PFC-NE system a useful tool for further scientific research in the ^{19}F MRI field, as NE can be prepared in a greater quantity ahead of time and then stored at −80 °C in small batches for cell or animal experiments. The production of larger batches without danger of wasting resources even renders batch characterization easier, making frequent testing of individual smaller batches unnecessary and streamlining the execution of *in-vitro* and *in-vivo* experiments. For larger experiment sets spanning several days or weeks, the storage-stability of these PFC-NE enables the use of a single batch of PFC-NE for the whole experiment without any loss in maleimide-functionality or droplet degradation, making the experiment results more comparable among each other and execution of experiments easier than with just-in-time manufacture of several PFC-NE. The NE modification system was even more reliable than the typically used PIT method, which displayed a more distinct variation in modification results, while this system is simultaneously more straightforward in use.

Acknowledgements

We thank Lipoid for supplying S75 and DSPE-mPEG(2000), Sabine Barnert for cryoTEM image acquisition and Marie Follo for proofreading.

References

[1] S. Temme, F. Bönner, J. Schrader, U. Flögel, 19F magnetic resonance imaging of endogenous macrophages in inflammation, Wiley Interdiscip. Rev. Nanomed. Nanobiotechnol. 4 (2012) 329–343, https://doi.org/10.1002/wnan.1163.
[2] S. Temme, C. Grapentin, C. Quast, C. Jacoby, M. Grandoch, Z. Ding, C. Owenier, F. Mayenfels, J.W. Fischer, R. Schubert, J. Schrader, U. Flögel, Noninvasive imaging of early venous thrombosis by 19F magnetic resonance imaging with targeted perfluorocarbon nanoemulsions clinical perspective, Circulation 131 (2015) 1405–1414, https://doi.org/10.1161/circulationaha.114.010962.
[3] P. Bouvain, V. Flocke, W. Krämer, R. Schubert, J. Schrader, U. Flögel, S. Temme, Dissociation of 19F and fluorescence signal upon cellular uptake of dual-contrast perfluorocarbon nanoemulsions, MAGMA 32 (2018) 133–145, https://doi.org/10.1007/s10334-018-0723-7.
[4] D. O'Hagan, Understanding organofluorine chemistry. An introduction to the C-F bond, Chem. Soc. Rev. 37 (2008) 308–319, https://doi.org/10.1039/B711844A.
[5] J.G. Riess, Oxygen carriers ("blood substitutes") - raison d'etre, chemistry, and some physiology, Chem. Rev. 101 (2001) 2797–2919, https://doi.org/10.1021/cr970143c.
[6] D.R. Spahn, K.F. Waschke, T. Standl, J. Motsch, L. Van Huynegem, M. Welte, H. Gombotz, P. Coriat, L. Verkh, S. Faithfull, P. Keipert, Use of perflubron emulsion to decrease allogeneic blood transfusion in high-blood-loss non-cardiac surgery results of a European phase 3 study, Anesthesiology 97 (2002) 1338–1349.
[7] S.F. Flaim, Pharmacokinetics and side effects of perfluorocarbon-based blood substitutes, Artif. Cells Blood Substit. Biotechnol. 22 (1994) 1043–1054, https://doi.org/10.3109/10731199409138801.
[8] B. Ebner, P. Behm, C. Jacoby, S. Burghoff, B.A. French, J. Schrader, U. Flögel, Early assessment of pulmonary inflammation by 19F MRI in vivo, Circ. Cardiovasc. Imaging 3 (2010) 202–210, https://doi.org/10.1161/circimaging.109.902312.
[9] S. Weibel, T.C. Basse-Luesebrink, M. Hess, E. Hofmann, C. Seubert, J. Langbein-Laugwitz, I. Gentschev, V.J.F. Sturm, Y. Ye, T. Kampf, P.M. Jakob, A.A. Szalay, Imaging of intratumoral inflammation during oncolytic virotherapy of tumors by 19F-magnetic resonance imaging (MRI), PLoS ONE 8 (2013) e56317, https://doi.org/10.1371/journal.pone.0056317.
[10] U. Flögel, S. Su, I. Kreideweiß, Z. Ding, L. Galbarz, J. Fu, C. Jacoby, O. Witzke, J. Schrader, Noninvasive detection of graft rejection by in vivo 19F MRI in the early stage: Early diagnosis of graft rejection by 19F MRI, Am. J. Transplant. 11 (2011) 235–244, https://doi.org/10.1111/j.1600-6143.2010.03372.x.
[11] U. Flögel, Z. Ding, H. Hardung, S. Jander, G. Reichmann, C. Jacoby, R. Schubert, J. Schrader, In vivo monitoring of inflammation after cardiac and cerebral ischemia by fluorine magnetic resonance imaging, Circulation 118 (2008) 140–148, https://doi.org/10.1161/CIRCULATIONAHA.107.737890.
[12] C. Jacoby, S. Temme, F. Mayenfels, N. Benoit, M.P. Krafft, R. Schubert, J. Schrader, U. Flögel, Probing different perfluorocarbons for in vivo inflammation imaging by 19 F MRI: image reconstruction, biological half-lives and sensitivity: Perfluorocarbons for in vivo inflammation imaging by 19F MRI, NMR Biomed. 27 (2014) 261–271, https://doi.org/10.1002/nbm.3059.
[13] M. Srinivas, P. Boehm-Sturm, C.G. Figdor, I.J. de Vries, M. Hoehn, Labeling cells for in vivo tracking using 19F MRI, Biomaterials 33 (2012) 8830–8840, https://doi.org/10.1016/j.biomaterials.2012.08.048.
[14] L. Lemaire, G. Bastiat, F. Franconi, N. Lautram, T. Duong Thi Dan, E. Garcion, P. Saulnier, J.P. Benoit, Perfluorocarbon-loaded lipid nanocapsules as oxygen sensors for tumor tissue pO2 assessment, Eur. J. Pharm. Biopharm. 84 (2013) 479–486, https://doi.org/10.1016/j.ejpb.2013.01.003.
[15] S. Ganta, A. Singh, N.R. Patel, J. Cacaccio, Y.H. Rawal, B.J. Davis, M.M. Amiji, T.P. Coleman, Development of EGFR-targeted nanoemulsion for imaging and novel platinum therapy of ovarian cancer, Pharm. Res. 31 (2014) 2490–2502, https://doi.org/10.1007/s11095-014-1345-z.
[16] S. Temme, P. Baran, P. Bouvain, C. Grapentin, W. Krämer, B. Knebel, H. Al-Hasani, J.M. Moll, D. Floss, J. Schrader, R. Schubert, U. Flögel, J. Scheller, Synthetic cargo internalization receptor system for nanoparticle tracking of individual cell populations by fluorine magnetic resonance imaging, ACS Nano 12 (2018) 11178–11192, https://doi.org/10.1021/acsnano.8b05698.
[17] S. Temme, C. Grapentin, T. Güden-Silber, U. Flögel, Chapter 4 Active targeting of perfluorocarbon nanoemulsions, in: U. Flögel, E. Ahrens (Eds.), Fluorine Magnetic Resonance Imaging, Pan Stanford Publishing, Pan Stanford Publishing Pte. Ltd., Penthouse Level, Suntec Tower 3, 8 Temasek Boulevard, Singapore 038988, 2016, pp. 103–140, , https://doi.org/10.1201/9781315364605-5.
[18] D.L. Iden, T.M. Allen, In vitro and in vivo comparison of immunoliposomes made by conventional coupling techniques with those made by a new post-insertion approach, BBA Biomembranes 1513 (2001) 207–216, https://doi.org/10.1016/S0005-2736(01)00357-1.
[19] M. Gantert, F. Lewrick, J.E. Adrian, J. Rössler, T. Steenpaß, R. Schubert, R. Peschka-Süss, Receptor-specific targeting with liposomes in vitro based on sterol-PEG1300 anchors, Pharm. Res. 26 (2008) 529, https://doi.org/10.1007/s11095-008-9768-z.
[20] D. Molnar, J. Linders, C. Mayer, R. Schubert, Insertion stability of poly(ethylene glycol)-cholesteryl-based lipid anchors in liposome membranes, Eur. J. Pharm. Biopharm. 103 (2016) 51–61, https://doi.org/10.1016/j.ejpb.2016.03.023.
[21] G.T. Hermanson, Heterobifunctional crosslinkers, Bioconjugate Techniques, Elsevier, 2013, pp. 299–339, , https://doi.org/10.1016/B978-0-12-382239-0.00006-6.
[22] J. Wang, S. Yang, K. Zhang, Multi-arm PEG-maleimide conjugation intermediate characterization and hydrolysis study by a selective HPLC method, J. Pharm. Biomed. Anal. 164 (2019) 452–459, https://doi.org/10.1016/j.jpba.2018.11.009.
[23] A.R. do V. Morais, É. do N. Alencar, F.H. Xavier Júnior, C.M. de Oliveira, H.R. Marcelino, G. Barratt, H. Fessi, E.S.T. do Egito, A. Elaissari, Freeze-drying of emulsified systems: A review, Int. J. Pharm. 503 (2016) 102–114, https://doi.org/10.1016/j.ijpharm.2016.02.047.
[24] M.G. Freire, A.M.A. Dias, M.A.Z. Coelho, J.A.P. Coutinho, I.M. Marrucho, Aging mechanisms of perfluorocarbon emulsions using image analysis, J. Colloid Interface Sci. 286 (2005) 224–232, https://doi.org/10.1016/j.jcis.2004.12.036.
[25] C. Grapentin, S. Barnert, R. Schubert, Monitoring the stability of perfluorocarbon nanoemulsions by cryo-TEM image analysis and dynamic light scattering, PLoS ONE 10 (2015) e0130674, https://doi.org/10.1371/journal.pone.0130674.
[26] J.M. Roe, B.W. Barry, Photon correlation spectroscopy of pharmaceutical systems (sodium dodecyl sulphate, sodium deoxycholate and chlorpromazine hydrochloride micelles and polystyrene latices), Int. J. Pharm. 14 (1983) 159–171, https://doi.org/10.1016/0378-5173(83)90091-1.
[27] G.T. Hermanson, Fluorescent probes, Bioconjugate Techniques, Elsevier, 2013, pp. 395–463, , https://doi.org/10.1016/B978-0-12-382239-0.00010-8.
[28] G.R. Bartlett, Phosphorus assay in column chromatography, J. Biol. Chem. 234 (1959) 466–468.
[29] K. Jores, W. Mehnert, M. Drechsler, H. Bunjes, C. Johann, K. Mader, Investigations on the structure of solid lipid nanoparticles (SLN) and oil-loaded solid lipid nanoparticles by photon correlation spectroscopy, field-flow fractionation and transmission electron microscopy, J. Control Release 95 (2004) 217–227.
[30] M. Holzer, S. Barnert, J. Momm, R. Schubert, Preparative size exclusion chromatography combined with detergent removal as a versatile tool to prepare unilamellar and spherical liposomes of highly uniform size distribution, J. Chromatogr. A. 1216 (2009) 5838–5848.
[31] J. Kuntsche, J.C. Horst, H. Bunjes, Cryogenic transmission electron microscopy (cryo-TEM) for studying the morphology of colloidal drug delivery systems, Int. J. Pharm, Adv. Characterizat. Tech. 417 (2011) 120–137, https://doi.org/10.1016/j.ijpharm.2011.02.001.
[32] D. Needham, T.J. McIntosh, D.D. Lasic, Repulsive interactions and mechanical stability of polymer-grafted lipid membranes, BBA Biomembranes 1108 (1992) 40–48, https://doi.org/10.1016/0005-2736(92)90112-Y.
[33] N. Dos Santos, C. Allen, A.-M. Doppen, M. Anantha, K.A.K. Cox, R.C. Gallagher, G. Karlsson, K. Edwards, G. Kenner, L. Samuels, M.S. Webb, M.B. Bally, Influence of poly(ethylene glycol) grafting density and polymer length on liposomes: Relating plasma circulation lifetimes to protein binding, BBA Biomembranes 1768 (2007) 1367–1377, https://doi.org/10.1016/j.bbamem.2006.12.013.